Title page

i. Title:

Springtime ecosystem-scale monoterpene fluxes from Mediterranean pine forests across a precipitation gradient

ii. Running head:

Monoterpene fluxes across a precipitation gradient

iii. List of authors:

Roger Seco[1], Thomas Karl[2], Andrew Turnipseed[3], Jim Greenberg[4], Alex Guenther[1], Joan Llusia[5,6], Josep Peñuelas[5,6], Uri Dicken[7], Eyal Rotenberg[7], Saewung Kim[1], Dan Yakir[7],

iv. Affiliations:

[1]{Department of Earth System Science, University of California, Irvine CA 92697, USA}

[2]{Institute of Atmospheric and Cryospheric Sciences, University of Innsbruck, Innsbruck, Austria}

[3]{2B Technologies, Inc., Boulder CO 80301, USA}

[4]{Atmospheric Chemistry Division, National Center for Atmospheric Research, Boulder CO 80301, USA}

[5]{CREAF, Cerdanyola del Vallès, 08193 Barcelona, Catalonia, Spain}

[6]{CSIC, Global Ecology Unit CREAF-CSIC-UAB, Cerdanyola del Vallès, 08193 Barcelona, Catalonia, Spain }

[7]{Earth and Planetary Sciences, Weizmann Institute of Science, Rehovot 76100, Israel}

v. Corresponding author:

Roger Seco (email@rogerseco.cat), Tel +1 9498245665, Fax +1 9498243874

vi. Keywords:

monoterpenes, drought, biogenic emissions, MEGAN, VOC, *Pinus halepensis*

vii. Type of article: Research paper

Abstract

We quantified springtime ecosystem-scale monoterpene fluxes from two similar Aleppo pine (*Pinus halepensis* Mill.) forests, located in Israel, that differed in the amount of received precipitation: Yatir in the arid south and Birya in the northern part of Israel (291 and 755 mm annual average rainfall, respectively). In addition to the lower water availability, during our measurement campaign the Yatir site suffered from a heat wave with temperatures up to 35 ºC, which made the campaign-average net CO_2 assimilation to occur in the morning (1 µmol m^{-2} s^{-1}), with the rest of the daytime hours mainly dominated by net release of CO_2. The milder conditions at Birya favored a higher net CO_2 assimilation during all daytime hours (with average peaks higher than 10 µmol m^{-2} s^{-1}). Despite these large differences in ambient conditions and CO_2 net assimilation, daytime monoterpene emission capacities at both sites were comparable. While observed monoterpene fluxes were lower at Yatir than at Birya (hourly averages up to 0.4 and 1 mg m^{-2} h^{-1}, respectively), the standardized hourly fluxes, after accounting for the differences in light, temperature and stand density between both sites, were comparable (0-1.3 mg m^{-2} h^{-1}). The approach typically used by biogenic emission models overestimated monoterpene fluxes at Yatir when temperatures rose during the heat wave. This result, together with complementary leaf-level measurements showing that summertime monoterpene fluxes almost completely ceased at Yatir while being enhanced at Birya, highlight the interaction of water scarcity and high temperatures that drive monoterpene emissions from vegetation in such extreme climate zones and the need to further improve model performance.

1. Introduction

Plants exchange hundreds of different volatile organic compounds (VOCs) with the atmosphere (Kesselmeier and Staudt, 1999; Park et al., 2013; Seco et al., 2007). On a global scale the emission flux of biogenic VOCs (BVOCs) is estimated to be an order of magnitude greater than that from anthropic sources (Guenther et al., 1995). BVOCs can substantially influence the composition and chemistry of the atmosphere, especially when interacting with anthropogenic pollutants (Atkinson, 2000; Chameides et al., 1988; Deventer et al., 2015; Kim et al., 2016; Liu et al., 2016; Seco et al., 2011b; Trainer et al., 1987; Tunved et al., 2006). Due to their atmospheric influence, BVOC fluxes are increasingly considered a necessary component of earth system models, and the response of modeled emissions to global change phenomena has been identified as a key uncertainty in these models (e.g., Müller *et al.*, 2008; Unger *et al.*, 2013; Sindelarova *et al.*, 2014). There is particular need for a better mechanistic understanding due to the increasing impact of drought (Dai, 2012) and other global-change-related stresses on BVOC emissions (Seco et al., 2015).

In addition, BVOCs have important biological and ecological roles such as acting as communication signals in plant–plant, plant–animal and multitrophic relationships (Baldwin et al., 2006; Filella et al., 2013; Kessler and Baldwin, 2001; Peñuelas et al., 2005a; Pichersky and Gershenzon, 2002; Seco et al., 2011a), or protecting vegetation from abiotic stresses (Peñuelas et al., 2005b; Singsaas and Sharkey, 1998; Velikova et al., 2005). Among abiotic stresses, drought and high temperatures often concur and subject plants to a slowdown of their metabolism (Hsiao, 1973), a reorganization of their energy resources (Dobrota, 2006), and eventually to increased mortality through the interaction of several mechanisms (e.g. sap cavitation, carbon starvation, biotic agents; Gaylord *et al.*, 2015). Plants have developed mechanisms to survive under hydric

stress by resisting, tolerating, or preventing it (Niinemets, 2010a). One of these mechanisms is the emission of BVOCs, particularly isoprenoids, that could provide the plant with relief against the damaging effect of drought and high temperatures (Loreto et al., 1998; Peñuelas and Llusia, 2003, 2002) and could eventually allow ecosystem stress to be quantified through BVOC flux monitoring (Kravitz et al., 2016). The responses of BVOC emissions to drought are nevertheless complex and depend, among other factors, on plant and BVOC species, ontogeny and previous acclimation, duration and strength of drought conditions, as well as the interaction with other biotic and abiotic stressors (Geron et al., 2016; Niinemets et al., 2010; Niinemets, 2010b).

Given the uncertainty in our knowledge of the response of BVOC emissions to drought, our objective in this study was to compare the exchange of BVOCs between two similar Mediterranean forests growing under different water availabilities. Israel presents a strong gradient in water availability, ranging from semi-arid conditions in the south to Mediterranean/sub-humid in the north. The aridity index (ratio of precipitation to potential evapotranspiration) in Israel lies between 0.05 in the south to above 0.65 in the north (Kafle and Bruins, 2009). The Aleppo pine (*Pinus halepensis* Mill.) is a widespread species with a large distribution around the Mediterranean basin (Critchfield and Little, 1966) and an estimated total forest cover of approximately 3.5 million ha (Fady et al., 2003). *P. halepensis* is known for being a fast grower, pioneer, and drought tolerant species with a shallow root system (Oppenheimer, 1967). These characteristics made it a favorable tree for plantations in the Mediterranean region, particularly in Israel. Its ability to withstand drought is enabled mainly by reducing growth rate and water loss. Water loss is minimized thanks to morphophysiological modifications of the leaves that are sclerotic and needle-shaped to minimize the leaf area and thus limit excessive transpiration, as well as by shifting photosynthetic activity to early morning and late afternoon

(Maseyk et al., 2008). The BVOC emissions of *P. halepensis* are dominated by monoterpenes (a family of isoprenoid hydrocarbons with a carbon skeleton of 10 atoms) and it has been reported that drought affects monoterpene (Llusià and Peñuelas, 2000, 1998) and other BVOC (Filella et al., 2009; Seco et al., 2008) emission rates of this particular tree species, as well as of other pine species (e.g. Trowbridge *et al.*, 2014; Eller *et al.*, 2016).

We quantified the ecosystem-level fluxes of monoterpenes from two similar 50-year-old Aleppo pine plantations in Israel that differ by nearly 500 mm in the amount of annual precipitation. Measurements at the ecosystem scale afford an integrated view of the forest monoterpene fluxes, reducing the influence of plant-to-plant variability, and also limit the impact of possible damage-induced emissions due to leaf manipulation during leaf-level sampling with enclosures, which has been the common measurement technique in past *P. halepensis* studies. In addition, our choice of pine plantations provided an opportunity to study the emission of BVOCs on mature trees under naturally occurring stresses, as opposed to performing laboratory experiments on young potted plants. Measurements of monoterpenes took place between 22 April and 13 May 2013 and were part of the BRITE (Biogeochemical Research along an Israeli TransEct) campaign, which aimed to investigate CO_2, H_2O, energy, VOC, and aerosol fluxes from pine forests along a precipitation gradient in this semi-arid region using a newly designed mobile flux measurement laboratory (see Asaf *et al.*, 2013).

2. Materials and methods

2.1. Description of the forest sites

The BRITE campaign focused on two mature plantations dominated by *P. halepensis* and located in Israel (Fig. 1). The drier forest, Yatir, is a ca. 50-year-old Aleppo pine afforestation site located at the northern edge of the Negev desert (31°20'N, 35°03'E) at an elevation of 650 m asl. The forest covers an area of about 2,800 ha and grows on a predominantly light brown Rendzina soil (79 ± 45.7 cm deep), overlying a chalk and limestone bedrock (http://www.kkl-jnf.org). The climate is hot (40-year mean annual temperature is 18.2°C) and dry (40-yr average mean annual precipitation is 291 mm). During the year of this study (October 2012-September 2013) the total precipitation was 247 mm. The precipitation and temperature data was derived from the Israeli Meteorological Service (IMS, https://ims.data.gov.il) permanent stations and values used are the average of the three closest stations to the measurement site. The Yatir forest is characterized by a low stand density of ca. 300 trees ha^{-1} (http://www.kkl-jnf.org), with a mean tree height of 10.2 m, a mean diameter at breast height (DBH) of 19.8 cm, and an average leaf area index (LAI) of 1.50 (Sprintsin et al., 2011). It has been a continuously operated Fluxnet site since 2000 (Rotenberg and Yakir, 2011; Tatarinov et al., 2016).

The second site, Birya, is a ca. 50-year-old planted forest covering approximately 2,000 ha in the northern Galilee region (33°00'N, 35°30'E, about 200 km north of Yatir) at an elevation of 755 m asl and is characterized by Rendzina and Terra rossa soil (http://www.kkl-jnf.org). Its climate is Mediterranean sub-humid with an average temperature and annual precipitation of 16°C and 755 mm, respectively (data derived from IMS stations as explained for Yatir). Between October 2012 and September 2013 the measured precipitation was 885 mm. Its average stand density is 375 trees ha^{-1} (http://www.kkl-jnf.org), the mean tree height is 11 m and its mean DBH is 20.3 cm.

Given that plantation age, mean tree height, and mean diameter at breast height are very similar between both forests, we estimated the LAI for the Birya site as the average LAI value of Yatir multiplied by the ratio of stand density between the two sites (375/300 = 1.25), i.e. a LAI value of 1.875.

2.2. Environmental and ecophysiological parameters

Measurements of the BRITE campaign at both sites primarily relied on the deployment of a newly designed mobile laboratory of the Weizmann Institute of Science, housed on a 12-ton four-wheel drive pneumatic air suspension truck frame. The mobile platform hosted a 28 m telescopic mast with a core (CO_2, H_2O, sensible and latent heat fluxes) eddy covariance (EC) system, and provided an air-conditioned enclosed facility for the operation of additional scientific instrumentation (e.g. Asaf *et al.*, 2013). The EC system centered on a 3D sonic anemometer (R3-100; Gill Instruments, UK) and an enclosed-path infrared gas analyzer (IRGA, LI-7200, LI-COR Inc, Lincoln, NE, USA). The core EC fluxes were averaged over 30 min time intervals with EddyPro v5.1 software (LI-COR Inc). Sensors for other environmental parameters, such as air pressure, temperature and relative humidity (HMP45C probes, Campbell Scientific Inc., UT, USA), and solar radiation (Kipp & Zonen, Delft, Netherlands) were also installed as part of the mobile EC system.

Some periods in the evening were excluded from data collected at Yatir (including monoterpene data), due to influence of a campfire (e.g. 22, 23, 25 April) that the site guards built. Additionally, at the Yatir site the permanent EC tower located in close proximity of the mobile platform during the BRITE campaign was used to assess and cross-calibrate the mobile EC system during April 2013.

166

167 *2.3. VOC measurements*

168 VOC measurements were performed with the same instrument setup installed in the mobile
169 laboratory, at both the Yatir forest (22 to 29 April 2013) and at the Birya forest (2 to 13 May
170 2013). Air from the top of the mobile tower (20 m agl), next to the sonic anemometer, was drawn
171 by means of a pump through a 3/8 inch OD (1/4 inch ID) PFA Teflon tube to the mobile lab
172 located at the base of the tower. VOC quantification was performed inside the mobile lab with a
173 high sensitivity Proton Transfer Reaction –Quadrupole– Mass Spectrometer (PTR-Quad-MS,
174 Ionicon, Austria) that has been described elsewhere (Karl et al., 2001). In short, the instrument
175 generates hydronium ions that transfer a proton to select VOC molecules in a drift tube under a
176 constant electric field (Lindinger et al., 1998). These charged VOC molecules are then detected
177 by the combined effect of a quadrupole mass spectrometer and an ion detector. The drift tube of
178 the instrument used in this study was operated at a pressure of 2.3 mbar, a temperature of 60 ºC
179 and a voltage of 540 V, corresponding to an E/N ratio of approximately 117 Td (E being the
180 electric field strength and N the gas number density; 1 Td = 10^{-17} V cm^2).

181 Instrument background was measured for 5 min every 6 h by diverting the inlet air through a
182 platinum catalytic converter heated to 380 ºC. Calibration of the PTR-MS was performed by
183 dilution of a house-made VOC gas standard into zero air generated by a second heated catalyst
184 (415 ºC). Two mass flow controllers (MKS Instruments, Andover MA, USA) were used for the
185 dilution. The gas standard contained approximately 5 ppmv of camphene. The calibration factors
186 measured for camphene were used to calculate the total monoterpene mixing ratios in ambient
187 air. The uncertainty of the monoterpene measurements was estimated to be 15%. The *m/z* (mass
188 to charge ratios) of interest for this study were *m/z* 21 (H_3O^+ isotope, 0.5 s dwell time), and *m/z*

81 and *m/z* 137 (monoterpene fragment and parent ions, respectively, 0.1 s dwell time each). The cycle scanning through all the measured *m/z* ratios had a duration of approximately 1.1 s (i.e., each *m/z* was measured once every 1.1 s), and measurements for EC were recorded for 25 min of each half hour. The monoterpene mixing ratio detection limit was <0.02 ppbv for each 25-min averaging period.

VOC fluxes were calculated with the virtual disjunct eddy covariance technique (vDEC; Karl *et al.*, 2002). The disjunct time series that was generated for each *m/z* every half hour was time-aligned with the vertical wind data from the sonic anemometer by shifting one time series relative to the other until the absolute maximum covariance between the two time series was determined. Using this procedure the time lag between the two measurements was found to be approximately 3 s. Previously, the wind data had been rotated according to the planar fit method (Wilczak et al., 2001). Computed monoterpene fluxes were excluded from further analysis if any of the following conditions occurred: (1) turbulence was low (u^*<0.15); (2) vertical wind rotation exceeded 5º; (3) results of the stationarity test (Foken et al., 2004) were higher than 30%, and (4) flux values were less than twice the flux detection limit. The flux detection limit was calculated according to the approaches of Spirig *et al.* (2005) and Billesbach (2011), and ranged between 0.02 and 0.2 mg m^{-2} h^{-1} at different times of the day. These conditions excluded 56% and 61% of the total half-hour EC fluxes calculated for monoterpenes at Yatir and Birya, respectively. Excluding small fluxes and periods of low turbulence and large wind rotations may bias our averaged diel flux profiles (Figs. 4b and 5b), particularly at night when turbulence is often below the threshold. In this regard, nighttime fluxes presented in this study should be viewed as upper limits and we will mainly focus our discussion on daytime results. High frequency losses due to the instrument gas exchange time in the drift tube were not corrected for

because comparison to temperature co-spectra showed that the contribution of high frequencies to fluxes was typically under 10%. vDEC calculations were performed with MATLAB software (Mathworks, Natick MA, USA). Hereinafter, we will refer to our measurement-based vDEC flux estimates as "measured" fluxes when comparing to the "standardized" and "modeled" fluxes (see section 2.4).

Since most monoterpenes are reactive with ozone, and ozone was not scrubbed from the inlet line, we estimated the impact of reactions with ozone on the calculated monoterpene fluxes. The delay-time from the inlet to the detector was on the order of only 2 s, so we estimated that at ambient ozone levels of 60 ppbv this would equate to a flux loss of less than 0.5% for γ-terpinene, one of the most reactive monoterpenes. Solid absorbent cartridge ambient air sampling at the Yatir field site indicated that the monoterpenes were dominated by α-pinene which suggests that the canopy loss rate, according to modeling results of Stroud *et al.* (2005), is about 10% assuming ozone concentrations of 60 ppbv.

2.4. VOC flux modeling

To allow a better comparison of monoterpene emission capacity between the two sites, the measured canopy-scale monoterpene fluxes were standardized with regards to both i) light and temperature and ii) stand density. First, the light and temperature standardization was performed with a big-leaf model approach (e.g. Geron *et al.*, 1997), which considers the canopy as a single multispecies layer of foliage. Thus, above-canopy photosynthetic active radiation (PAR) instead of leaf-level PAR, and above-canopy air temperature instead of leaf temperature were used in the leaf-level algorithms developed by Guenther and colleagues (1999, 1993, 1991) to model the light- and temperature-dependent emission of monoterpenes. The light- and temperature-

standardized emission of monoterpenes (ε_{MT}; mg m^{-2} h^{-1}) was calculated from the measured monoterpene emission flux (F_{MT}; mg m^{-2} h^{-1}):

$$F_{MT} = \varepsilon_{MT} \times \gamma_P \times \gamma_T \quad (1)$$

where γ_P and γ_T are light and temperature activity factors, respectively, defined as

$$\gamma_P = (1 - LDF) + LDF \times \gamma_{P\_LDF} \quad (2)$$

$$\gamma_T = (1 - LDF) \times \gamma_{T\_LIF} + LDF \times \gamma_{T\_LDF} \quad (3)$$

Monoterpene emissions include a light-dependent fraction (*LDF*) with the remaining light independent fraction (*LIF*=1-*LDF*) that is not influenced by light. Since leaf-level measurements at Yatir showed that approximately half of the monoterpene emissions were triggered by light (Llusia et al., 2016), we used an *LDF* of 0.5. The light and temperature algorithms are defined as

$$\gamma_{P\_LDF} = \frac{\alpha \times C_{L1} \times L}{\sqrt{1 + \alpha^2 \times L^2}} \quad (4)$$

where γ_{P_LDF} is a scalar representing electron transport rates to simulate the response (non-dimensional) of isoprene emission to light (Guenther et al., 1991), α (=0.0027) and C_{L1} (=1.066) are empirical parameters, and L is PAR (µmol m^{-2} s^{-1}),

$$\gamma_{T\_LDF} = \frac{E_{opt} \times C_{T2} \times e^{C_{T1} \times x}}{C_{T2} - C_{T1} \times (1 - e^{C_{T2} \times x})}, \; x = \frac{\frac{1}{T_{opt}} - \frac{1}{T}}{R} \quad (5)$$

where γ_{T_LDF} is a scalar representing an enzyme activation to simulate the response (non-dimensional) of isoprene emission to temperature (Guenther et al., 1991), E_{opt} (=1.9 nmol m^{-2} s^{-1}) is the maximum standardized emission capacity at temperature T_{opt} (=312.5 K), C_{T1} (=80 kJ mol^{-1}) and C_{T2} (=230 kJ mol^{-1}) are empirical parameters, T is the air temperature (K) and R is the ideal gas constant (=0.008314 kJ K^{-1} mol^{-1}), and

$$\gamma_{T\_LIF} = e^{\beta \times (T - T_{ref})} \quad (6)$$

where T_{ref} equals 303.15 K and β (=0.1 K^{-1}) is an empirically determined coefficient with the value recommended for monoterpenes by Guenther *et al.* (2012). Secondly, the stand density standardization consisted of dividing the light- and temperature-standardized fluxes of the Birya site by 1.25, viz. the ratio of stand density between the two sites, the same approach used to estimate the LAI of Birya.

As an additional modeling experiment, monoterpene fluxes at both sites were estimated with a single location version of the widely-used MEGAN version 2.1 model (Guenther et al., 2012) that includes an explicit canopy environment model with a canopy radiation transfer and energy balance scheme to calculate direct and diffuse light and leaf temperature of sun and shade leaves at each of five layers. The model calculates fluxes as the product of a fixed canopy emission factor and non-dimensional emission activity factors. For this study, we used the model's global default canopy emission factor assigned to pine forests for monoterpenes, with a value of 2.25 mg m^{-2} h^{-1} based on whole canopy fluxes measured above pine forests (Holzinger et al., 2006; Kaser et al., 2013; Räisänen et al., 2009). The environmental conditions measured at the tower (air temperature, solar radiation, wind speed, etc) and the LAI of each site (i.e. 1.5 and 1.875 for Yatir and Birya, respectively) were used to constrain the driving variables of the model's emission activity factors. The temperature and light emission activity factors also included the influence of the past 24 h of temperature and light conditions. Unlike Yatir, that had the fixed tower data available, the influence of the past 240 h could not be computed for Birya due to insufficient data since the mobile laboratory was deployed only several hours before the PTR-MS measurements were started at that site. Using the past 240 h algorithm with Yatir's fixed tower data showed maximum modeled hourly monoterpene emission flux increases of 15-25%.

For the sake of comparability between sites, the influence of the past 240 h was not included in the modeling results of either site.

3. Results

3.1. Environmental conditions

During the weeks preceding our measurements at Yatir, maximum daily temperatures reached up to 20 ºC (data not shown). Starting around 23 April, a heat wave (see Tatarinov *et al.*, 2016) affected the area and maximum daily temperatures at Yatir raised up to 35 ºC (Fig. 2). As a consequence, vapor pressure deficit (VPD) also gradually increased from below 1 kPa to above 4 kPa (Fig. 2). At Birya, temperatures during our sampling period reached maxima around 30 ºC, then progressively declined as the heat wave ended, and VPD was in general lower than at Yatir, with occasional peaks around 3.7 kPa and declining with time to maxima of below 1 kPa (Fig. 2).

The comparison of hourly averages calculated for the entire campaign dataset shows that temperatures and VPD were higher (up to 4 ºC and 1.4 kPa more, respectively) at Yatir than at Birya (Fig. 3). Solar radiation was also higher on average (up to 200 W m^{-2} more, i.e. approximately 420 µmol m^{-2} s^{-1} more of PAR) during the middle of the day at Yatir (Fig. 3). This was in spite of the relatively close proximity (less than 200 km) and reflects the higher cloudiness in the northern site.

3.2. Water and carbon dioxide fluxes

Daytime canopy-level water flux measured at Yatir was lower than at Birya (Fig. 2). At both sites the highest water fluxes occurred in the morning between 8 and 13 h, with average values of 1.5-1.9 and 4-5.5 mmol m^{-2} s^{-1} for Yatir and Birya, respectively (Fig. 3). During the afternoon, water fluxes declined gradually until sunset.

During daytime hours before the onset of the heat wave, net ecosystem exchange (NEE) of CO_2 mainly consisted of assimilation at Yatir. The half-hour CO_2 assimilation peaks were as high as 10 µmol m^{-2} s^{-1}, similar to what is shown in Fig. 2 for 22 April. From April 23, daytime CO_2 NEE showed a tendency towards net emission (with occasional half-hour emission peaks of 6-8 µmol m^{-2} s^{-1}) with net CO_2 assimilation being limited to the 6-9 h morning time frame and to magnitudes of up to 2 µmol m^{-2} s^{-1} (Fig. 2). At Birya, daytime carbon assimilation was the norm, with a general temporal trend of an increase from daytime half-hour net CO_2 uptake maxima around 10 µmol m^{-2} s^{-1}, at the beginning, to around 20 µmol m^{-2} s^{-1} at the end of the campaign (Fig. 2).

Hourly averages of CO_2 fluxes calculated for the entire campaign dataset show that CO_2 NEE presented two daily assimilation peaks at both sites (Fig. 3). At Yatir, the morning peak of assimilation occurred between 6 and 9 h with magnitudes of approximately 1 µmol m^{-2} s^{-1}, whereas the afternoon peak of approximately 0.5 µmol m^{-2} s^{-1} occurred between 16 and 17 h. Between these two peaks, a mid-day depression in NEE consisted of CO_2 release to the atmosphere of up to 2.7 µmol m^{-2} s^{-1} (Fig. 3). At Birya, hourly average peaks of net assimilation of approximately 13 µmol m^{-2} s^{-1} occurred between 8 and 10 h and between 12 and 13 h, with a small decrease of approximately 2 µmol m^{-2} s^{-1} between both peaks (Fig. 3). Nighttime NEE at both forests was characterized by CO_2 release (i.e. ecosystem respiration) of approximately 2-4 µmol m^{-2} s^{-1} (Fig. 3). The aggregate of these CO_2 NEE fluxes over 24 h yields a daily average carbon release of 2 g(C) m^{-2} and absorption of 3.8 g(C) m^{-2} at Yatir and Birya, respectively.

3.3. Measured VOC fluxes and mixing ratios

Monoterpene mixing ratios were lower at Yatir than at Birya, with half-hour maxima of 0.2 and 1.2 ppbv, respectively (Fig. 2). Hourly averages show a daily trend at Yatir with minimum values recorded around 3-5 h (approximately 0.09 ppbv) and maxima during the evening (approximately 0.16 ppbv), although mixing ratios between 5 and 23 h varied within a narrow range (0.12-.0.16 ppbv) (Fig. 4). Measurements at Birya revealed a clearer diurnal cycle, with higher values from 6 to 13 h (0.24-0.32 ppbv) and minima during nighttime (0.12-0.16 ppbv) (Fig. 4).

Half-hour canopy-level fluxes of monoterpenes measured at Yatir were at or below 0.5 mg m^{-2} h^{-1} during daytime, with occasional peaks of up to 0.6 mg m^{-2} h^{-1}. At Birya canopy fluxes were generally higher, between 0.5 and 1 mg m^{-2} h^{-1}, with some peaks reaching 1.9 mg m^{-2} h^{-1} (Fig. 2). Consequently, hourly averages at Yatir between 6 and 18 h ranged between 0.3 and 0.4 mg m^{-2} h^{-1}, while at Birya monoterpene average fluxes were similar to those of Yatir during early morning and afternoon but higher between 9 and 13 h, with values of up to 1 mg m^{-2} h^{-1} (Fig. 4). Birya's net emission flux decreased after 16 h to the point that the average monoterpene net flux during several hours resulted in deposition (Fig. 4).

The 24-h total carbon emitted in the form of monoterpenes was, on average, 4.7 and 6 mg(C) m^{-2} at Yatir and Birya, respectively. Thus, since the daily average net carbon exchange had different sign between sites, the carbon emitted as monoterpenes equaled 0.24% of the net daily release of carbon as CO_2 at Yatir, while at Birya it represented 0.16% of the net daily carbon assimilation.

3.4. Modeled VOC fluxes

Adjusting for light intensity and temperature at Yatir, and for light and temperature and stand density at Birya, resulted in standardized (for a temperature of 30 ºC, PAR of 1000 µmol m^{-2} s^{-1}, and stand density of 300 trees ha^{-1}) fluxes that were generally higher than the measured fluxes (Fig. 4) primarily because temperatures were typically below 30 ºC at both sites (Figs. 2 and 3). Average standardized fluxes at Yatir were highest immediately after sunrise (1.3-2.1 mg m^{-2} h^{-1}), although the highest value (found between 7 and 8 h) was based only on one data point from the morning of 23 April, when temperatures were not yet fully affected by the regional heat wave. For the remainder of the daylight hours, average standardized fluxes at Yatir were in the range 0.5-1 mg m^{-2} h^{-1} (Fig. 4). Birya's standardized fluxes also increased, compared to the observed values, in the early morning up to 1.1 mg m^{-2} h^{-1} but were still highest around 9 h with average values of up to 1.3 mg m^{-2} h^{-1}. For most of the remainder of the daylight hours, average standardized fluxes at Birya were in the range of 0-1.3 mg m^{-2} h^{-1} (Fig. 4). Thus the average standardized monoterpene fluxes at both pine forests spanned a similar range (0-1.3 mg m^{-2} h^{-1}).

Results from the application of the MEGANv2.1 model, using a global default emission factor for pine trees, are compared to our measurements in Fig. 5. The model slightly underestimated monoterpene fluxes at Yatir during the first days of the campaign. During the heat wave, modeled fluxes overestimated the observed fluxes by as much as a factor of two on 28 April. As a result, the hourly averages calculated for the entire campaign dataset indicate that MEGAN, using default pine emission factors, predicted higher monoterpene emissions at Yatir from 8 to 16 h, also doubling the measured fluxes from 12 to 14 h (Fig. 5). If the influence of the past 10 days is included in the model calculations for Yatir (data not shown), monoterpene predicted emissions are increased by approximately 20%, which might partly reconcile the model results

and the observations during the first days, but exacerbates the overestimation of the MEGAN model during the hottest days of the heat wave. MEGAN's predictions for Birya reflected the day-to-day variation of the magnitude of the emissions better than for Yatir (Fig. 5). However, Birya's average observed fluxes gradually increased until they peaked between 10 and 11 h (1 mg m^{-2} h^{-1}) and gradually declined afterwards, while the model predicted emissions of monoterpenes continued to increase later in the day and showed a plateau from 10 to 13h (0.65-0.71 mg m^{-2} h^{-1}). As a result, modeled monoterpene fluxes were higher than measured until sunset at Birya (Fig. 5).

4. Discussion

The Yatir semi-arid pine afforestation system experienced harsher conditions for plant growth than the similar pine forest in Birya, as expected. Furthermore, the typical seasonal heat wave (Tatarinov et al., 2016) that affected the region at the end of April 2013 exacerbated the environmental conditions, as exemplified by the high VPD, low water fluxes, and practically zero daytime NEE (Figs. 2 and 3). Limitation of water loss is an important adaptive strategy of plants in this region, with the observed reduction of NEE being consistent with reports of strong reductions in stomatal conductance, and hence photosynthesis, at VPD > 2 kPa in *P. halepensis* trees located at Yatir (Klein et al., 2011; Maseyk et al., 2008). Despite the harsh environmental conditions at the Yatir site, this forest has successfully adapted by shifting the growing season such that it can assimilate carbon in annual amounts comparable to other temperate forests found in more favorable environments (Grunzweig et al., 2003; Maseyk et al., 2008) and also shows a great resilience to seasonal heat waves (Tatarinov et al., 2016).

Monoterpene emissions from different plant species occur at least through two distinct processes: in a light-independent manner from storage pools found in specialized tissues like resin ducts, and as a light-dependent release of freshly synthesized molecules. It has been traditionally thought that conifer trees emit monoterpenes mainly from storage pools even though there were reports of a strong light response of emissions of some monoterpenes from conifers including the Mediterranean stone pine, *Pinus pinea* (Staudt et al., 1997). Isotope labeling studies have recently been used to confirm that *de novo* light-dependent monoterpenes can comprise a significant fraction of emissions from European conifers in laboratory studies (Ghirardo et al., 2010) and under field conditions for the North American species *Pinus ponderosa* (Harley et al., 2014). The existence in *P. halepensis* of this dual path of monoterpene emissions was

corroborated during our field campaign with leaf-level measurements at Yatir, showing that about half of the emitted monoterpenes were driven by the incident PAR intensity (Llusia et al., 2016). Furthermore, our ecosystem-level data supports the prevalent role of light-dependent emissions since daytime monoterpene mixing ratios were higher than at nighttime at both sites (Fig. 4). In ecosystems where monoterpene emissions mainly follow a temperature controlled release from storage pools, the nighttime mixing ratios are higher due to decreased vertical mixing and oxidation rates even though emissions are also lower (e.g., Seco *et al.*, 2013; Davison *et al.*, 2009).

During the heat wave, monoterpene net emission fluxes at Yatir persisted during daytime even though the net CO_2 flux showed very small assimilation or mainly consisted of CO_2 efflux (Figs. 2-4). Apparently, part of this monoterpene emission consisted of light-independent releases from storage pools. But contribution from *de novo* light-dependent emissions, as has been shown from plant species that do not store monoterpenes, cannot be ruled out despite the intensely reduced net CO_2 assimilation. Isoprenoid emission concurrent with reduced photosynthesis has been described in previous studies and our dataset could be yet another example of the uncoupling between photosynthesis and isoprenoid emissions that occurs under stressful environmental conditions (e.g. Seco *et al.*, 2015; Wu *et al.*, 2015). Continued monoterpene emissions from leaves with limited stomatal conductance may happen through the cuticle but are also possible via the stomata due to their high gas to water partitioning coefficient that makes most biogenic isoprenoid emissions practically insensitive to stomatal closure (Harley, 2013; Niinemets and Reichstein, 2003). In addition, these isoprenoids emitted under stress, if freshly synthesized, can obtain their carbon supply from metabolic sources other than the recent photosynthate pool (Affek and Yakir, 2003; Brilli et al., 2007; Funk et al., 2004). The fact that monoterpenes are

emitted, sometimes even in increased amounts, during drought situations have been postulated to be a response of the plants to cope with high temperatures that usually accompany drought episodes (Loreto et al., 1998). In contrast, the pine trees at Birya showed no signs of strong water stress during our campaign, although water and CO_2 fluxes showed a midday depression that can be indicative of some level of mild water or VPD stress (Haldimann et al., 2008; Pathre et al., 1998). Likewise, the emission of monoterpenes was equivalent to only a small fraction of the assimilated carbon (up to 0.2% of NEE) at Birya, which is a relatively low amount compared to the percentage of carbon emitted as BVOC reported elsewhere for severely drought-stressed forests (e.g. up to 5-10% of NEE emitted as isoprene by high-emitting, non-storing temperate oak forests; Seco *et al.*, 2015).

The MEGANv2.1 model, when using a global average pine emission factor and partitioning of stored (light independent) and *de novo* (light dependent) emissions, did not accurately reproduce the monoterpene fluxes at Yatir (Fig. 5). During the first days of the campaign, the midday model results were similar to measurements but the diel pattern was not reproduced. After the onset of the heat wave the model clearly overestimated the emissions, mainly due to the higher temperatures driving the model's temperature response algorithms. At Birya, modeled emission magnitudes were in general closer to measurements (Fig. 5). However, the measured diel cycle showed a decline of monoterpene net emission fluxes earlier in the day compared to the model (Fig. 5), with observed monoterpene fluxes mirroring the diel water fluxes rather than the daily temperature trend (Figs. 3 and 4). This suggests a more prevalent role of *de novo* light-driven monoterpene synthesis and emission than assumed by MEGAN, and consequently a smaller role of the temperature-driven emissions of stored monoterpenes. As earlier stated, the fact that monoterpene mixing ratios were higher during daytime at both sites (Fig. 4) agrees with this

interpretation. In addition, the leaf-level measurements at Yatir also indicated that the monoterpene emissions from these Aleppo pines were partly driven by the incident PAR intensity (Llusia et al., 2016), and thus it is likely that the trees at Birya responded in a similar way. We did not have soil water content data for our campaign, even though this type of information is critical to help us understand BVOC emissions in the context of drought stress. Soil water content data can improve MEGAN's modeling results by the use of its simple drought algorithm, although recent results show that even when soil moisture data is available there is still room for model improvement (Seco et al., 2015) and that atmospheric demand for water can make VPD more limiting for ecosystem functioning than soil moisture supply (Novick et al., 2016). Furthermore, novel findings suggest that emissions of monoterpenes from pine oleoresin storage pools may also be regulated by the xylem water potential and not only by the ambient temperature and light conditions (Rissanen et al., 2016). These facts highlight the need for comprehensive availability of environmental and physiological information in order to gain insight into our physiological understanding and improve our BVOC emission modeling capability. It is especially relevant in the case of drought because limited water availability, particularly in areas like the Mediterranean, usually occurs during the summer when temperatures are also high. As a consequence, current air quality models could overestimate the BVOC emissions used as inputs for their predictions, leading to inaccurate results.

Our study shows that, despite the differences in environmental aridity between sites, both *P. halepensis* populations showed comparable monoterpene emission capacities during the spring season, as indicated by our standardized ecosystem-level eddy covariance results (Fig. 4c) and also by the leaf-level enclosure measurements reported by Llusia et al (2016). Leaf-level data available for the summer season, however, shows that monoterpene emissions at Yatir almost

ceased while at Birya, with more favorable conditions in terms of aridity, they increased 5-fold (Llusia et al., 2016). This site contrast emphasizes the role of water availability in regulating monoterpene emissions and its interactions with temperature. With sufficient water supply monoterpene emissions increase with temperature, while under severe drought stress the emissions are severely reduced.

Acknowledgements

RS was partly supported by a postdoctoral fellowship awarded by Fundación Ramón Areces. TK was supported by the EC Seventh Framework Program (Marie Curie Reintegration Program, "ALP-AIR", grant no. 334084). JP and JL acknowledge funding from the European Research Council Synergy grant ERC-2013-SyG-610028 IMBALANCE-P, the Spanish Government grant CGL2013-48074-P and the Catalan Government grant SGR 2014-274. Help by Dr. Pawel Misztal with computer programming was greatly appreciated. The National Center for Atmospheric Research is sponsored by the National Science Foundation. This work was supported by the Cathy Wills and Robert Lewis Program in Environmental Science, the KKL-JNF, and the Sussman Center of the Weizmann Institute of Science.

References

Affek, H.P., Yakir, D., 2003. Natural abundance carbon isotope composition of isoprene reflects incomplete coupling between isoprene synthesis and photosynthetic carbon flow. Plant Physiol. 131, 1727–36. doi:10.1104/pp.102.012294

Asaf, D., Rotenberg, E., Tatarinov, F., Dicken, U., Montzka, S.A., Yakir, D., 2013. Ecosystem photosynthesis inferred from measurements of carbonyl sulphide flux. Nat. Geosci. 6, 186–190. doi:10.1038/ngeo1730

Atkinson, R., 2000. Atmospheric chemistry of VOCs and NOx. Atmos. Environ. 34, 2063–2101. doi:10.1016/S1352-2310(99)00460-4

Baldwin, I.T., Halitschke, R., Paschold, A., von Dahl, C.C., Preston, C.A., 2006. Volatile signaling in plant-plant interactions: "Talking trees" in the genomics era. Science (80-.). 311, 812–815. doi:10.1126/science.1118446

Billesbach, D.P., 2011. Estimating uncertainties in individual eddy covariance flux measurements: A comparison of methods and a proposed new method. Agric. For. Meteorol. 151, 394–405. doi:10.1016/j.agrformet.2010.12.001

Brilli, F., Barta, C., Fortunati, A., Lerdau, M., Loreto, F., Centritto, M., 2007. Response of isoprene emission and carbon metabolism to drought in white poplar (Populus alba) saplings. New Phytol. 175, 244–54. doi:10.1111/j.1469-8137.2007.02094.x

Chameides, W., Lindsay, R., Richardson, J., Kiang, C., 1988. The role of biogenic hydrocarbons in urban photochemical smog: Atlanta as a case study. Science (80-.). 241, 1473–1475. doi:10.1126/science.3420404

Critchfield, W.B., Little, E.L.J., 1966. Geographic distribution of the pines of the world. USDA, Forest Service, Miscellaneous publication 991.

Dai, A., 2012. Increasing drought under global warming in observations and models. Nat. Clim. Chang. 3, 52–58. doi:10.1038/nclimate1633

Davison, B., Taipale, R., Langford, B., Misztal, P., Fares, S., Matteucci, G., Loreto, F., Cape, J.N., Rinne, J., Hewitt, C.N., 2009. Concentrations and fluxes of biogenic volatile organic compounds above a Mediterranean macchia ecosystem in western Italy. Biogeosciences 6, 1655–1670. doi:10.5194/bg-6-1655-2009

Deventer, M.J., Held, A., El-Madany, T.S., Klemm, O., 2015. Size-resolved eddy covariance fluxes of nucleation to accumulation mode aerosol particles over a coniferous forest. Agric. For. Meteorol. 214–215, 328–340. doi:10.1016/j.agrformet.2015.08.261

Dobrota, C., 2006. Energy dependant plant stress acclimation. Rev. Environ. Sci. Bio/Technology 5, 243–251. doi:10.1007/s11157-006-0012-1

Eller, A.S.D., Young, L.L., Trowbridge, A.M., Monson, R.K., 2016. Differential controls by climate and physiology over the emission rates of biogenic volatile organic compounds from mature trees in a semi-arid pine forest. Oecologia 180, 345–358. doi:10.1007/s00442-015-3474-4

Fady, B., Semerci, H., Vendramin, G., 2003. EUFORGEN Technical Guidelines for genetic conservation and use for Aleppo pine (*Pinus halepensis*) and Brutia pine (*Pinus brutia*). Rome, Italy.

Filella, I., Peñuelas, J., Seco, R., 2009. Short-chained oxygenated VOC emissions in *Pinus halepensis* in response to changes in water availability. Acta Physiol. Plant. 31, 311–318. doi:10.1007/s11738-008-0235-6

Filella, I., Primante, C., Llusià, J., Martín González, A.M., Seco, R., Farré-Armengol, G., Rodrigo, A., Bosch, J., Peñuelas, J., 2013. Floral advertisement scent in a changing plant-pollinators market. Sci. Rep. 3, 3434. doi:10.1038/srep03434

Foken, T., Göockede, M., Mauder, M., Mahrt, L., Amiro, B., Munger, W., 2004. Post-Field Data Quality Control, in: Lee, X., Massman, W., Law, B. (Eds.), Handbook of Micrometeorology. Kluwer Academic Publishers, Dordrecht, Netherlands, pp. 181–208. doi:10.1007/1-4020-2265-4_9

Funk, J.L., Mak, J.E., Lerdau, M.T., 2004. Stress-induced changes in carbon sources for isoprene production in Populus deltoides. Plant, Cell Environ. 27, 747–755. doi:10.1111/j.1365-3040.2004.01177.x

Gaylord, M.L., Kolb, T.E., McDowell, N.G., 2015. Mechanisms of piñon pine mortality after severe drought: a retrospective study of mature trees. Tree Physiol. 35, 806–16. doi:10.1093/treephys/tpv038

Geron, C., Daly, R., Harley, P., Rasmussen, R., Seco, R., Guenther, A., Karl, T., Gu, L., 2016. Large drought-induced variations in oak leaf volatile organic compound emissions during PINOT NOIR 2012. Chemosphere 146, 8–21. doi:10.1016/j.chemosphere.2015.11.086

Geron, C.D., Nie, D., Arnts, R.R., Sharkey, T.D., Singsaas, E.L., Vanderveer, P.J., Guenther, A., Sickles, J.E., Kleindienst, T.E., 1997. Biogenic isoprene emission: Model evaluation in a southeastern United States bottomland deciduous forest. J. Geophys. Res. 102, 18889. doi:10.1029/97JD00968

Ghirardo, A., Koch, K., Taipale, R., Zimmer, I., Schnitzler, J.-P., Rinne, J., 2010. Determination of de novo and pool emissions of terpenes from four common boreal/alpine trees by 13 CO 2 labelling and PTR-MS analysis. Plant. Cell Environ. 33, 781–792. doi:10.1111/j.1365-3040.2009.02104.x

Grunzweig, J.M., Lin, T., Rotenberg, E., Schwartz, A., Yakir, D., 2003. Carbon sequestration in arid-land forest. Glob. Chang. Biol. 9, 791–799. doi:10.1046/j.1365-2486.2003.00612.x

Guenther, A., Baugh, B., Brasseur, G., Greenberg, J., Harley, P., Klinger, L., Serça, D., Vierling, L., 1999. Isoprene emission estimates and uncertainties for the central African EXPRESSO study domain. J. Geophys. Res. 104, 30625. doi:10.1029/1999JD900391

Guenther, A., Hewitt, C.N., Erickson, D., Fall, R., Geron, C., Graedel, T., Harley, P., Klinger, L., Lerdau, M., Mckay, W.A., Pierce, T., Scholes, B., Steinbrecher, R., Tallamraju, R., Taylor, J., Zimmerman, P., 1995. A global model of natural volatile organic compound emissions. J. Geophys. Res. 100, 8873. doi:10.1029/94JD02950

Guenther, A., Zimmerman, P.R., Harley, P., Monson, R.K., Fall, R., 1993. Isoprene and

568 Monoterpene Emission Rate Variability - Model Evaluations and Sensitivity Analyses. J.
569 Geophys. Res. 98, 12609–12617.

570 Guenther, A.B., Jiang, X., Heald, C.L., Sakulyanontvittaya, T., Duhl, T., Emmons, L.K., Wang,
571 X., 2012. The Model of Emissions of Gases and Aerosols from Nature version 2.1
572 (MEGAN2.1): an extended and updated framework for modeling biogenic emissions.
573 Geosci. Model Dev. 5, 1471–1492. doi:10.5194/gmd-5-1471-2012

574 Guenther, A.B., Monson, R.K., Fall, R., 1991. Isoprene and monoterpene emission rate
575 variability: Observations with eucalyptus and emission rate algorithm development. J.
576 Geophys. Res. 96, 10799. doi:10.1029/91JD00960

577 Haldimann, P., Galle, A., Feller, U., 2008. Impact of an exceptionally hot dry summer on
578 photosynthetic traits in oak (Quercus pubescens) leaves. Tree Physiol. 28, 785–795.
579 doi:10.1093/treephys/28.5.785

580 Harley, P., Eller, A., Guenther, A., Monson, R.K., 2014. Observations and models of emissions
581 of volatile terpenoid compounds from needles of ponderosa pine trees growing in situ:
582 control by light, temperature and stomatal conductance. Oecologia 176, 35–55.
583 doi:10.1007/s00442-014-3008-5

584 Harley, P.C., 2013. The Roles of Stomatal Conductance and Compound Volatility in Controlling
585 the Emission of Volatile Organic Compounds from Leaves, in: Niinemets, Ü., Monson,
586 R.K. (Eds.), Biology, Controls and Models of Tree Volatile Organic Compound Emissions.
587 pp. 181–208. doi:10.1007/978-94-007-6606-8_7

588 Holzinger, R., Lee, A., McKay, M., Goldstein, A.H., 2006. Seasonal variability of monoterpene
589 emission factors for a ponderosa pine plantation in California. Atmos. Chem. Phys. 6,
590 1267–1274. doi:10.5194/acp-6-1267-2006

591 Hsiao, T.C., 1973. Plant Responses to Water Stress. Annu. Rev. Plant Physiol. 24, 519–570.
592 doi:10.1146/annurev.pp.24.060173.002511

593 Kafle, H.K., Bruins, H.J., 2009. Climatic trends in Israel 1970–2002: warmer and increasing
594 aridity inland. Clim. Change 96, 63–77. doi:10.1007/s10584-009-9578-2

595 Karl, T., Guenther, A., Jordan, A., Fall, R., Lindinger, W., 2001. Eddy covariance measurement
596 of biogenic oxygenated VOC emissions from hay harvesting. Atmos. Environ. 35, 491–495.

597 Karl, T., Spirig, C., Rinne, J., Stroud, C., Prevost, P., Greenberg, J., Fall, R., Guenther, A., 2002.
598 Virtual disjunct eddy covariance measurements of organic compound fluxes from a
599 subalpine forest using proton transfer reaction mass spectrometry. Atmos. Chem. Phys. 2,
600 279–291.

601 Kaser, L., Karl, T., Guenther, A., Graus, M., Schnitzhofer, R., Turnipseed, A., Fischer, L.,
602 Harley, P., Madronich, M., Gochis, D., Keutsch, F.N., Hansel, A., 2013. Undisturbed and
603 disturbed above canopy ponderosa pine emissions: PTR-TOF-MS measurements and
604 MEGAN 2.1 model results. Atmos. Chem. Phys. 13, 11935–11947. doi:10.5194/acp-13-
605 11935-2013

606 Kesselmeier, J., Staudt, M., 1999. Biogenic volatile organic compounds (VOC): An overview on
607 emission, physiology and ecology. J. Atmos. Chem. 33, 23–88.

608 doi:10.1023/A:1006127516791

609 Kessler, A., Baldwin, I.T., 2001. Defensive function of herbivore-induced plant volatile
610 emissions in nature. Science (80-.). 291, 2141–2144.

611 Kim, S., Sanchez, D., Wang, M., Seco, R., Jeong, D., Hughes, S., Barletta, B., Blake, D.R., Jung,
612 J., Kim, D., Lee, G., Lee, M., Ahn, J., Lee, S.-D., Cho, G., Sung, M.-Y., Lee, Y.-H., Kim,
613 D.B., Kim, Y., Woo, J.-H., Jo, D., Park, R., Park, J.-H., Hong, Y.-D., Hong, J.-H., 2016.
614 OH reactivity in urban and suburban regions in Seoul, South Korea – an East Asian
615 megacity in a rapid transition. Faraday Discuss. 189, 231–251. doi:10.1039/C5FD00230C

616 Klein, T., Cohen, S., Yakir, D., 2011. Hydraulic adjustments underlying drought resistance of
617 *Pinus halepensis*. Tree Physiol. 31, 637–648. doi:10.1093/treephys/tpr047

618 Kravitz, B., Guenther, A.B., Gu, L., Karl, T., Kaser, L., Pallardy, S.G., Peñuelas, J., Potosnak,
619 M.J., Seco, R., 2016. A new paradigm of quantifying ecosystem stress through chemical
620 signatures. Ecosphere 7, e01559. doi:10.1002/ecs2.1559

621 Lindinger, W., Hansel, A., Jordan, A., 1998. On-line monitoring of volatile organic compounds
622 at pptv levels by means of proton-transfer-reaction mass spectrometry (PTR-MS) - Medical
623 applications, food control and environmental research. Int. J. Mass Spectrom. 173, 191–241.

624 Liu, Y., Brito, J., Dorris, M.R., Rivera-Rios, J.C., Seco, R., Bates, K.H., Artaxo, P., Duvoisin, S.,
625 Keutsch, F.N., Kim, S., Goldstein, A.H., Guenther, A.B., Manzi, A.O., Souza, R.A.F.,
626 Springston, S.R., Watson, T.B., McKinney, K.A., Martin, S.T., 2016. Isoprene
627 photochemistry over the Amazon rainforest. Proc. Natl. Acad. Sci. 113, 6125–6130.
628 doi:10.1073/pnas.1524136113

629 Llusià, J., Peñuelas, J., 2000. Seasonal patterns of terpene content and emission from seven
630 Mediterranean woody species in field conditions. Am. J. Bot. 87, 133–140.
631 doi:10.2307/2656691

632 Llusià, J., Peñuelas, J., 1998. Changes in terpene content and emission in potted Mediterranean
633 woody plants under severe drought. Can. J. Bot. 76, 1366–1373. doi:10.1139/b98-141

634 Llusia, J., Roahtyn, S., Yakir, D., Rotenberg, E., Seco, R., Guenther, A., Peñuelas, J., 2016.
635 Photosynthesis, stomatal conductance and terpene emission response to water availability in
636 dry and mesic Mediterranean forests. Trees 30, 749–759. doi:10.1007/s00468-015-1317-x

637 Loreto, F., Forster, A., Durr, M., Csiky, O., Seufert, G., 1998. On the monoterpene emission
638 under heat stress and on the increased thermotolerance of leaves of Quercus ilex L.
639 fumigated with selected monoterpenes. Plant, Cell Environ. 21, 101–107.
640 doi:10.1046/j.1365-3040.1998.00268.x

641 Maseyk, K.S., Lin, T., Rotenberg, E., Grünzweig, J.M., Schwartz, A., Yakir, D., 2008.
642 Physiology-phenology interactions in a productive semi-arid pine forest. New Phytol. 178,
643 603–16. doi:10.1111/j.1469-8137.2008.02391.x

644 Müller, J.-F., Stavrakou, T., Wallens, S., De Smedt, I., Van Roozendael, M., Potosnak, M.J.,
645 Rinne, J., Munger, B., Goldstein, A., Guenther, A.B., 2008. Global isoprene emissions
646 estimated using MEGAN, ECMWF analyses and a detailed canopy environment model.
647 Atmos. Chem. Phys. 8, 1329–1341. doi:10.5194/acp-8-1329-2008

Niinemets, Ü., 2010a. Responses of forest trees to single and multiple environmental stresses from seedlings to mature plants: Past stress history, stress interactions, tolerance and acclimation. For. Ecol. Manage. 260, 1623–1639. doi:10.1016/j.foreco.2010.07.054

Niinemets, Ü., 2010b. Mild versus severe stress and BVOCs: thresholds, priming and consequences. Trends Plant Sci. 15, 145–153. doi:10.1016/j.tplants.2009.11.008

Niinemets, Ü., Arneth, A., Kuhn, U., Monson, R.K., Peñuelas, J., Staudt, M., 2010. The emission factor of volatile isoprenoids: stress, acclimation, and developmental responses. Biogeosciences 7, 2203–2223. doi:10.5194/bg-7-2203-2010

Niinemets, Ü., Reichstein, M., 2003. Controls on the emission of plant volatiles through stomata: Differential sensitivity of emission rates to stomatal closure explained. J. Geophys. Res. 108, 4208. doi:10.1029/2002JD002620

Novick, K.A., Ficklin, D.L., Stoy, P.C., Williams, C.A., Bohrer, G., Oishi, A.C., Papuga, S.A., Blanken, P.D., Noormets, A., Sulman, B.N., Scott, R.L., Wang, L., Phillips, R.P., 2016. The increasing importance of atmospheric demand for ecosystem water and carbon fluxes. Nat. Clim. Chang. 6, 1023–1027. doi:10.1038/nclimate3114

Oppenheimer, H.R., 1967. Mechanisms of drought resistance in conifers of the Mediterranean zone and the arid west of the U.S.A. Part I: Physiological and Anatomical investigations. Final Report on project No. A10−FS 7, Grant No. FG−Is−119e. The Hebrew University of Jerusalem, Faculty of Agriculture, Rehovot, Israel.

Park, J.-H., Goldstein, A.H., Timkovsky, J., Fares, S., Weber, R., Karlik, J., Holzinger, R., 2013. Active Atmosphere-Ecosystem Exchange of the Vast Majority of Detected Volatile Organic Compounds. Science (80-.). 341, 643–647. doi:10.1126/science.1235053

Pathre, U., Sinha, A.K., Shirke, P.A., Sane, P. V., 1998. Factors determining the midday depression of photosynthesis in trees under monsoon climate. Trees 12, 472. doi:10.1007/s004680050177

Peñuelas, J., Filella, I., Stefanescu, C., Llusia, J., 2005a. Caterpillars of Euphydryas aurinia (Lepidoptera: Nymphalidae) feeding on Succisa pratensis leaves induce large foliar emissions of methanol. New Phytol. 167, 851–857.

Peñuelas, J., Llusia, J., 2003. BVOCs: plant defense against climate warming? Trends Plant Sci. 8, 105–109.

Peñuelas, J., Llusia, J., 2002. Linking photorespiration, monoterpenes and thermotolerance in Quercus. New Phytol. 155, 227–237.

Peñuelas, J., Llusia, J., Asensio, D., Munné-Bosch, S., 2005b. Linking isoprene with plant thermotolerance, antioxidants and monoterpene emissions. Plant Cell Environ. 28, 278–286.

Pichersky, E., Gershenzon, J., 2002. The formation and function of plant volatiles: perfumes for pollinator attraction and defense. Curr. Opin. Plant Biol. 5, 237–243.

Räisänen, T., Ryyppö, A., Kellomäki, S., 2009. Monoterpene emission of a boreal Scots pine (*Pinus sylvestris* L.) forest. Agric. For. Meteorol. 149, 808–819. doi:10.1016/j.agrformet.2008.11.001

687 Rissanen, K., Hölttä, T., Vanhatalo, A., Aalto, J., Nikinmaa, E., Rita, H., Bäck, J., 2016. Diurnal
688 patterns in Scots pine stem oleoresin pressure in a boreal forest. Plant. Cell Environ. 39,
689 527–538. doi:10.1111/pce.12637

690 Rotenberg, E., Yakir, D., 2011. Distinct patterns of changes in surface energy budget associated
691 with forestation in the semiarid region. Glob. Chang. Biol. 17, 1536–1548.
692 doi:10.1111/j.1365-2486.2010.02320.x

693 Seco, R., Filella, I., Llusia, J., Peñuelas, J., 2011a. Methanol as a signal triggering isoprenoid
694 emissions and photosynthetic performance in *Quercus ilex*. Acta Physiol. Plant. 33, 2413–
695 2422. doi:10.1007/s11738-011-0782-0

696 Seco, R., Karl, T., Guenther, A., Hosman, K.P., Pallardy, S.G., Gu, L., Geron, C., Harley, P.,
697 Kim, S., 2015. Ecosystem-scale volatile organic compound fluxes during an extreme
698 drought in a broadleaf temperate forest of the Missouri Ozarks (central USA). Glob. Chang.
699 Biol. 21, 3657–3674. doi:10.1111/gcb.12980

700 Seco, R., Peñuelas, J., Filella, I., 2008. Formaldehyde emission and uptake by Mediterranean
701 trees Quercus ilex and Pinus halepensis. Atmos. Environ. 42, 7907–7914.
702 doi:10.1016/j.atmosenv.2008.07.006

703 Seco, R., Peñuelas, J., Filella, I., 2007. Short-chain oxygenated VOCs: Emission and uptake by
704 plants and atmospheric sources, sinks, and concentrations. Atmos. Environ. 41, 2477–2499.
705 doi:10.1016/j.atmosenv.2006.11.029

706 Seco, R., Peñuelas, J., Filella, I., Llusià, J., Molowny-Horas, R., Schallhart, S., Metzger, A.,
707 Müller, M., Hansel, A., 2011b. Contrasting winter and summer VOC mixing ratios at a
708 forest site in the Western Mediterranean Basin: the effect of local biogenic emissions.
709 Atmos. Chem. Phys. 11, 13161–13179. doi:10.5194/acp-11-13161-2011

710 Seco, R., Peñuelas, J., Filella, I., Llusia, J., Schallhart, S., Metzger, A., Müller, M., Hansel, A.,
711 2013. Volatile organic compounds in the western Mediterranean basin: urban and rural
712 winter measurements during the DAURE campaign. Atmos. Chem. Phys. 13, 4291–4306.
713 doi:10.5194/acp-13-4291-2013

714 Sindelarova, K., Granier, C., Bouarar, I., Guenther, A., Tilmes, S., Stavrakou, T., Müller, J.-F.,
715 Kuhn, U., Stefani, P., Knorr, W., 2014. Global data set of biogenic VOC emissions
716 calculated by the MEGAN model over the last 30 years. Atmos. Chem. Phys. 14, 9317–
717 9341. doi:10.5194/acp-14-9317-2014

718 Singsaas, E.L., Sharkey, T.D., 1998. The regulation of isoprene emission responses to rapid leaf
719 temperature fluctuations. Plant Cell Environ. 21, 1181–1188.

720 Spirig, C., Neftel, A., Ammann, C., Dommen, J., Grabmer, W., Thielmann, A., Schaub, A.,
721 Beauchamp, J., Wisthaler, A., Hansel, A., 2005. Eddy covariance flux measurements of
722 biogenic VOCs during ECHO 2003 using proton transfer reaction mass spectrometry.
723 Atmos. Chem. Phys. 5, 465–481. doi:10.5194/acp-5-465-2005

724 Sprintsin, M., Cohen, S., Maseyk, K., Rotenberg, E., Grünzweig, J., Karnieli, A., Berliner, P.,
725 Yakir, D., 2011. Long term and seasonal courses of leaf area index in a semi-arid forest
726 plantation. Agric. For. Meteorol. 151, 565–574. doi:10.1016/j.agrformet.2011.01.001

Staudt, M., Bertin, N., Hansen, U., Seufert, G., Ciccioli, P., Foster, P., Frenzel, B., Fugit, J.-L., 1997. Seasonal and diurnal patterns of monoterpene emissions from Pinus pinea (L.) under field conditions. Atmos. Environ. 31, 145–156. doi:10.1016/S1352-2310(97)00081-2

Stroud, C., Makar, P., Karl, T., Guenther, A., Geron, C., Turnipseed, A., Nemitz, E., Baker, B., Potosnak, M., Fuentes, J.D., 2005. Role of canopy-scale photochemistry in modifying biogenic-atmosphere exchange of reactive terpene species: Results from the CELTIC field study. J. Geophys. Res. 110, D17303. doi:10.1029/2005JD005775

Tatarinov, F., Rotenberg, E., Maseyk, K., Ogée, J., Klein, T., Yakir, D., 2016. Resilience to seasonal heat wave episodes in a Mediterranean pine forest. New Phytol. 210, 485–496. doi:10.1111/nph.13791

Trainer, M., Williams, E.J., Parrish, D.D., Buhr, M.P., Allwine, E.J., Westberg, H.H., Fehsenfeld, F.C., Liu, S.C., 1987. Models and observations of the impact of natural hydrocarbons on rural ozone. Nature 329, 705–707. doi:10.1038/329705a0

Trowbridge, A.M., Daly, R.W., Helmig, D., Stoy, P.C., Monson, R.K., 2014. Herbivory and climate interact serially to control monoterpene emissions from pinyon pine forests. Ecology 95, 1591–1603. doi:10.1890/13-0989.1

Tunved, P., Hansson, H.C., Kerminen, V.M., Strom, J., Dal Maso, M., Lihavainen, H., Viisanen, Y., Aalto, P.P., Komppula, M., Kulmala, M., 2006. High natural aerosol loading over boreal forests. Science (80-.). 312, 261–263. doi:10.1126/science.1123052

Unger, N., Harper, K., Zheng, Y., Kiang, N.Y., Aleinov, I., Arneth, A., Schurgers, G., Amelynck, C., Goldstein, A., Guenther, A., Heinesch, B., Hewitt, C.N., Karl, T., Laffineur, Q., Langford, B., A. McKinney, K., Misztal, P., Potosnak, M., Rinne, J., Pressley, S., Schoon, N., Serça, D., 2013. Photosynthesis-dependent isoprene emission from leaf to planet in a global carbon-chemistry-climate model. Atmos. Chem. Phys. 13, 10243–10269. doi:10.5194/acp-13-10243-2013

Velikova, V., Pinelli, P., Pasqualini, S., Reale, L., Ferranti, F., Loreto, F., 2005. Isoprene decreases the concentration of nitric oxide in leaves exposed to elevated ozone. New Phytol. 166, 419–426.

Wilczak, J.M., Oncley, S.P., Stage, S.A., 2001. Sonic Anemometer Tilt Correction Algorithms. Boundary-Layer Meteorol. 99, 127–150. doi:10.1023/A:1018966204465

Wu, C., Pullinen, I., Andres, S., Carriero, G., Fares, S., Goldbach, H., Hacker, L., Kasal, T., Kiendler-Scharr, A., Kleist, E., Paoletti, E., Wahner, A., Wildt, J., Mentel, T.F., 2015. Impacts of soil moisture on de novo monoterpene emissions from European beech, Holm oak, Scots pine, and Norway spruce. Biogeosciences 12, 177–191. doi:10.5194/bg-12-177-2015

Figure legends

Fig. 1. Map showing the location of our two pine forest sites: Yatir in the south, Birya in the north of Israel. The base map image is from Google Earth (image and data copyright: Google, US Dept of State Geographer, Landsat, SIO, NOAA, US Navy, NGA, GEBCO).

Fig. 2. Half-hour data of environmental and physiological parameters (solar radiation and temperature, top panel; water flux and vapor pressure deficit, second panel; net CO_2 ecosystem exchange, third panel), and monoterpene (MT) mixing ratios and canopy-level fluxes (bottom panel) measured at the two sites: Yatir (left) and Birya (right). Date labels indicate 00:00 h Israel Standard Time (UTC +2 h).

Fig. 3. Hourly averaged diel cycles of the environmental and physiological parameters measured at the two pine forests: temperature (a), solar radiation (b), net water flux (c), vapor pressure deficit (d), and net CO_2 ecosystem exchange (e). Error bars indicate plus or minus one standard deviation for each hourly average.

Fig. 4. Hourly averaged diel cycles of the monoterpene (MT) mixing ratios (a, top panel), measured MT fluxes (b, middle panel), and standardized MT fluxes (c, bottom panel). Nighttime measured fluxes should be viewed as upper limits and are colored lighter in panel b. Standardized fluxes were computed to account for light, temperature, and tree density differences between sites (see section 2.4 for details) and only when PAR > 150 μmol m^{-2} s^{-1}. Error bars indicate plus or minus one standard deviation for each hourly average.

Fig. 5. Comparison of half-hour data (a) and hourly averaged diel cycles (b) of canopy-level monoterpene (MT) fluxes between the measurements and the MEGAN model results for each

site. Nighttime measured fluxes should be viewed as upper limits and are colored lighter in panel b. Error bars in panel b indicate plus or minus one standard deviation for each hourly average.

788 **Figures**

789 Fig 1.

790

791

792 Fig. 2

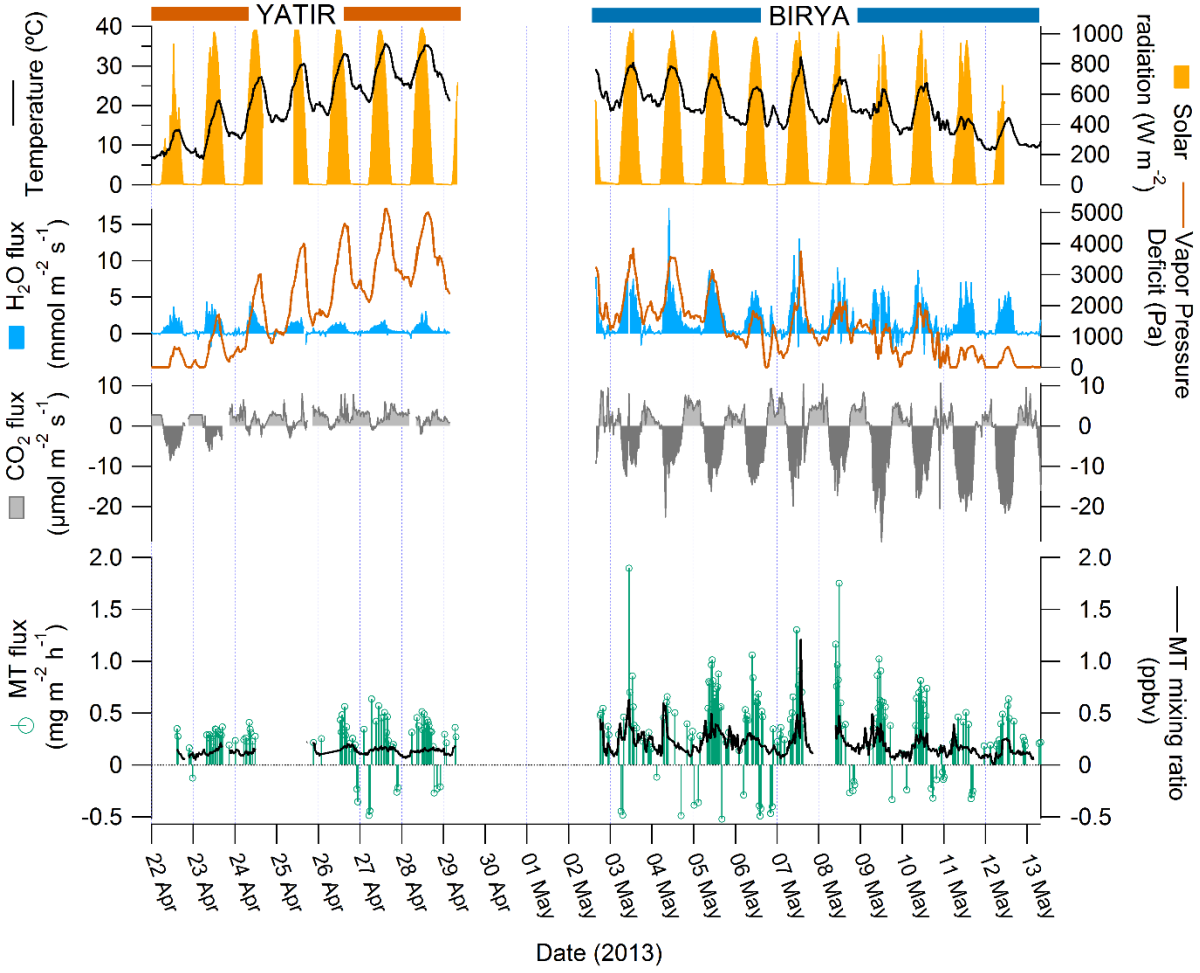

793

794

795 Fig 3.

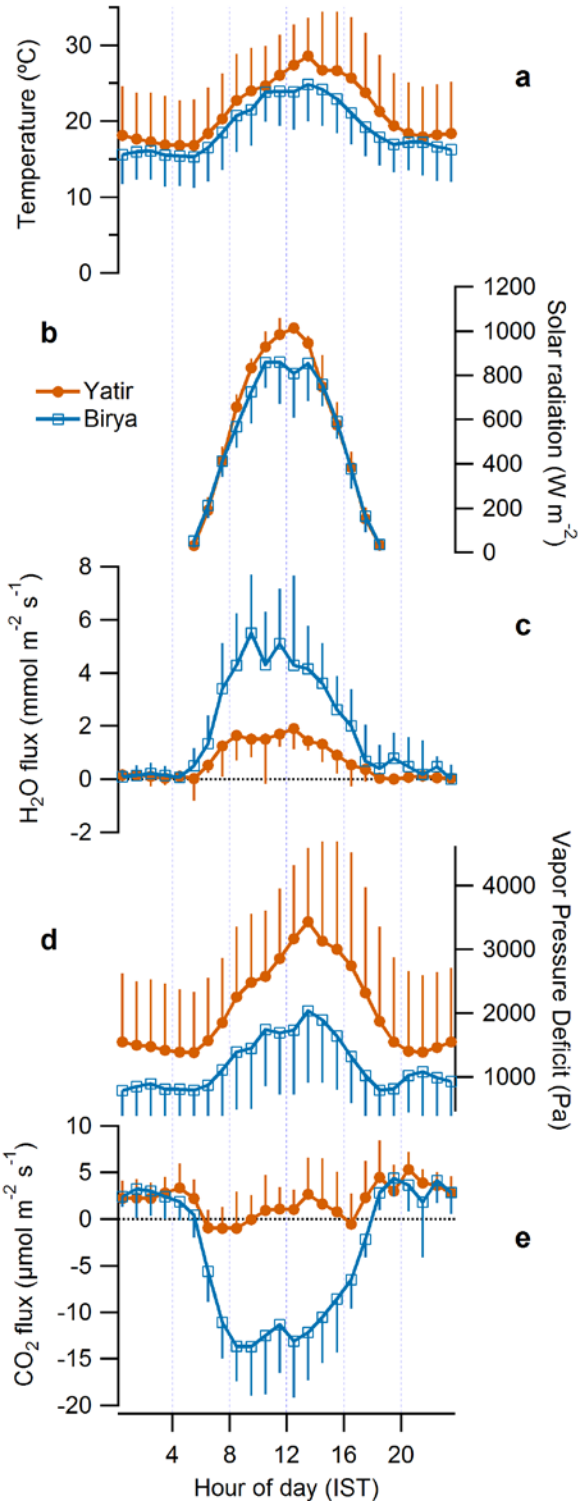

796
797
798

799 Fig 4.

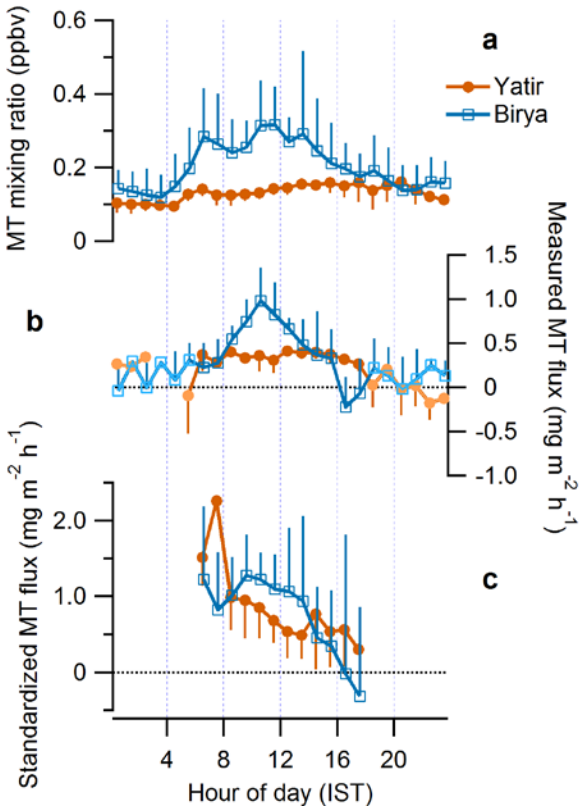

800

801

802

803

804 Fig 5.

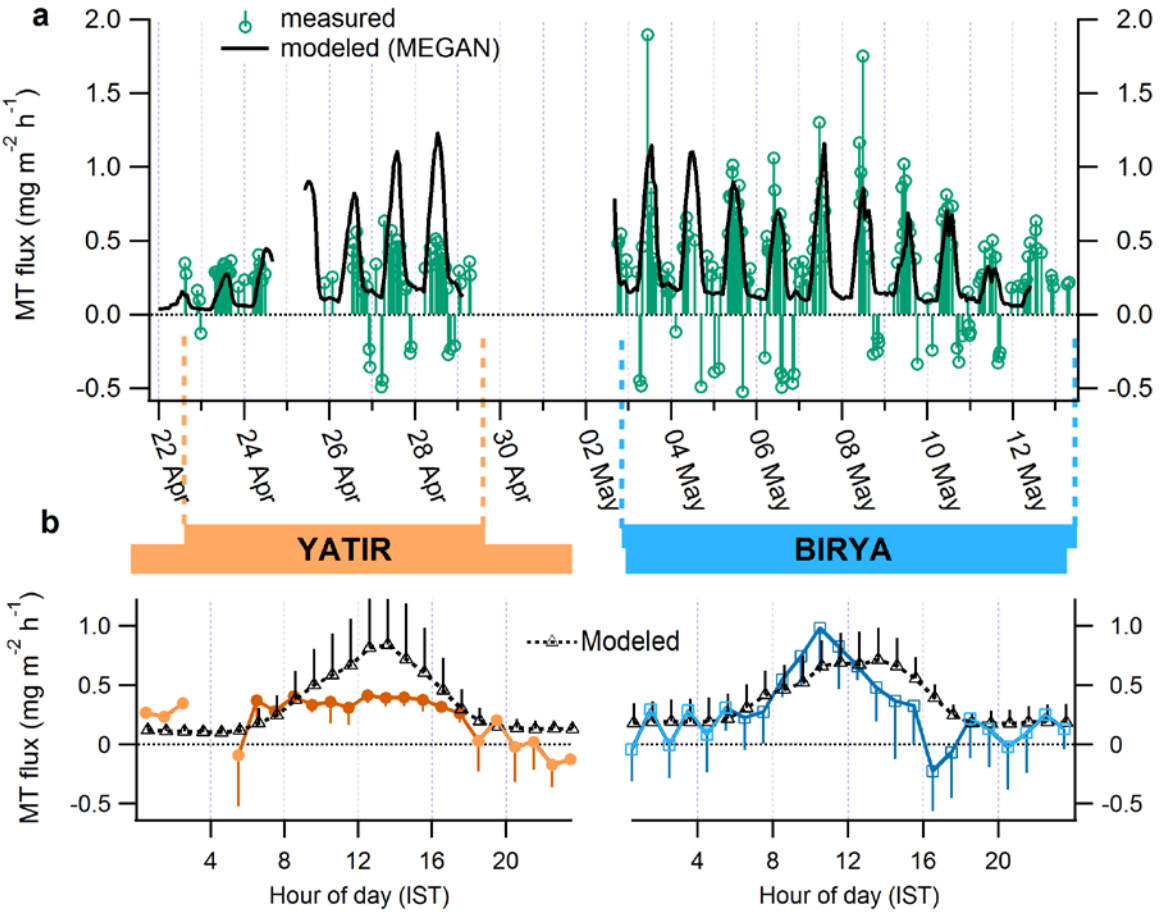

805

806